

RESEARCH

Open Access



Butyrate inhibits histone deacetylase 2 expression to alleviate liver fibrosis in biliary atresia

Yilin Zhao^{1,2†}, Xiaodan Xu^{3†}, Shaowen Liu^{1,2}, Xueting Wang⁴, Jiayinaxi Musha^{1,2,5}, Tengfei Li^{1,2}, Liang Ge², Yan Sun², Shujian Zhang², Li Zhao⁶ and Jianghua Zhan^{2*}

Abstract

Background Previous studies have found a reduction in butyrate-producing bacteria in the gut microbiota of infants with biliary atresia (BA). Butyrate is also an important inhibitor of histone deacetylase 2 (HDAC2). This study aims to explore how butyrate alleviates liver fibrosis in BA through HDAC2.

Methods Fibrosis-related pathways associated with butyrate were analyzed using the GSE46960 database. BA liver sections were used to validate factor expression. The effects of HDAC2 and butyrate and the pathway were performed in vitro experiments. Butyrate intervention was performed in bile duct ligation (BDL) mice, and alterations in the gut microbiota were analyzed using fecal 16S rRNA sequencing. The impact of butyrate and related pathways on liver fibrosis in BDL mice was further evaluated.

Results The IL-6/STAT3 pathway showed a clear correlation with butyrate in BA. HDAC2 promoted LX-2 activation via the IL-6/STAT3 pathway, while butyrate inhibited LX-2 activation by suppressing HDAC2. Butyrate not only alleviated liver fibrosis but also improved the gut microbiota structure in BDL mice.

Conclusion Butyrate may improve liver fibrosis in BA by regulating HDAC2 expression and modulating the IL-6/STAT3 pathway. Therefore, butyrate could serve as a promising therapeutic option for mitigating liver fibrosis in BA.

Keywords Biliary atresia, Fibrosis, Butyrate, HDAC2, IL-6, STAT3

[†]Yilin Zhao and Xiaodan Xu contributed equally as co-first authors.

*Correspondence:

Jianghua Zhan
zhanjianghuatj@163.com

¹Graduate College, Tianjin Medical University, Tianjin, China

²Department of General Surgery, Tianjin Children's Hospital, LongYan Road 238, Beichen District, Tianjin 300134, P. R. China

³Department of Pediatric Surgery, Tongji Hospital, Tongji Medical College, Huazhong University of Science and Technology, Wuhan, Hubei Province, China

⁴Department of Pediatric Surgery, Xinjiang Yili Friendship Hospital, Yili, China

⁵Department of Pediatric Surgery, Urumqi First People's Hospital (Urumqi Children's Hospital), Xinjiang, China

⁶Department of Pathology, Tianjin Children's Hospital, Tianjin, China

Introduction

Biliary atresia (BA) is a leading cause of neonatal cholestasis and a serious life-threatening condition [1]. BA is characterized by progressive inflammation and fibrosis of the biliary tract, with an incidence ranging from 1 in 5,000 to 1 in 20,000 [2, 3]. The exact cause of BA remains unclear [4, 5, 6, 7]. Hepaticojejunal anastomosis (Kasai) is the procedure of choice for the treatment of BA, utilizing Roux-en-Y anastomosis to restore bile drainage and relieve obstruction. However, after Kasai's surgery, some of the infants still had progressive liver fibrosis and eventually a liver transplant to save their lives [8]. Early and rapidly progressive liver fibrosis is an important factor



leading to poor native liver survival (NLS) in BA. Identifying its potential mechanisms of development is key to effectively controlling the progression of liver fibrosis and extending the time of NLS.

Some research has demonstrated that the gut microbiota, a key element of the “gut-liver axis”, plays a direct or indirect role in influencing both the structure and function of the liver [9, 10]. Under normal conditions, the gut microbiota and the host maintain a mutually beneficial symbiosis and the microecological stability under the joint barrier effect of secretory mucus, intestinal epithelial cells, and the immune microenvironment [11]. However, liver disease disrupts this balance, leading to gut microbiota alterations. It has been found that the balance are significantly altered in BA, and the number of *Bifidobacteria* and butyric acid-producing flora is significantly reduced [12]. Butyrate, a type of short-chain fatty acid (SCFA) generated through the metabolic activity of gut microbiota, is essential for supporting intestinal well-being and modulating immune system activity. We also found that butyrate-producing *Firmicutes* were significantly reduced in BA patients [13]. As a product of related microbiota, butyrate may have a beneficial impact on the prognosis of BA.

Histone acetylation and deacetylation are crucial components of the epigenetics of diseases. Histone acetylation, a reversible epigenetic modification, is closely associated with the activation of gene transcription, whereas histone deacetylation typically represses transcriptional activity [14]. The opposing functions of two enzymes, histone acetyltransferases (HATs) and histone deacetylases (HDACs), control the equilibrium. HDACs are key regulators in the activation of hepatic stellate cells (HSCs) [15]. Butyrate, an important endogenous HDAC inhibitor, interacts with HDACs to regulate gene expression and cell proliferation [16]. Butyrate can alleviate the progression of non-alcoholic fatty liver disease (NAFLD) and hepatitis, suppress liver inflammation, and slow down liver fibrosis [17]. In earlier studies, we found reduced butyrate levels and elevated HDAC2 expression in infants with BA, both of which were correlated with BA-related liver fibrosis [13, 18]. Building on these findings, we propose that butyrate can inhibit HSC activation and mitigate the progression of liver fibrosis in BA by the downregulation of HDAC2 expression.

Methods

Human sample

To evaluate the expression of relevant factors, liver tissue samples were obtained from 10 infants diagnosed with type III BA, while 8 infants with choledochal cysts (CC) served as disease controls (DCs). All diagnoses were confirmed by intraoperative cholangiography, and liver tissue samples were obtained during surgery. Sections of

liver tissue were utilized for conducting histological and immunohistochemical staining analyses (Supplementary material 1).

Cell lines

LX-2 were purchased from Procell Life Science&Technology Co.,Ltd, Wuhan. Cells were cultured in DMEM, 10% fetal bovine serum and 1% penicillin and streptomycin. The cells were maintained in a controlled environment at 37 °C with 5% CO₂. ITSA-1 (Inhibitor Trichostatin A-1, HDAC activators, hereafter referred to as ITSA), sodium butyrate (hereafter referred to as BU) was added to the medium of LX-2 cells. WP1066 (MedChemExpress, NewJersey) was used to specifically inhibit JAK/STAT3 signaling pathway in LX-2. HDAC2 expression in HSCs was knocked down using siRNA, with a blank control group (Con) and a siRNA non-targeting control group (si-NC) included for comparison. Total RNA and protein were extracted, followed by analysis using quantitative PCR (qPCR) and western blot (WB) (Supplementary material 1).

Mice module

6-8w male Balb/c mice were obtained from Vital River Laboratories (Beijing, China). The experimental animals were randomly assigned to three groups, each consisting of six mice: the bile duct ligation (BDL) group, the Sham group, and the BDL + sodium butyrate (BU) group. In the BDL + BU group, mice were administered BU (0.3 mg/g) via gavage once per day after common bile duct ligation. The Sham and BDL groups were administered an equivalent volume of saline via gavage once per day. Tissue samples were collected from all animals after 10 days post-surgery.

Mice are anesthetized via intraperitoneal injection of tribromoethanol and placed in a supine position with their limbs secured to the operating platform. A mid-line abdominal incision was made to expose the hepatic hilum, then isolated the common bile duct. The duct was ligated at both the proximal and distal ends using 8–0 sutures, and then severed between the two sutures. The abdominal contents are then repositioned, and the incision is closed. Liver, serum samples and feces were collected subsequently.

Histological staining

Wedge biopsy specimens of the liver were collected intraoperatively, fixed in formalin and embedded in paraffin to make 4 μm sections. Each histological section included at least ten hepatic lobules and was routinely stained using hematoxylin–eosin (HE), Masson’s trichrome and Sirius red. Fibrosis grade was assessed using the Metavir score for all Section [18]. All slides were reviewed by two senior pathologists and the difference of opinion was solved by a

common consensus. The observers were unaware of the clinical data. In this study, stage 1 and stage 2 fibrosis in BA patients were defined as mild fibrosis, while stage 3 and stage 4 fibrosis were defined as severe fibrosis.

Cell scratch assay

On the bottom of a 6-well plate, draw lines 1 cm apart. Seed 5×10^5 cells/well into the 6-well plate. Place the plate in a cell culture incubator and culture until the cell density reaches approximately 90%. Use a sterile pipette tip to make vertical scratches. Wash away non-adherent cells with PBS buffer and then take photographs under a microscope. Afterward, add the intervention drug to the culture medium and continue culturing. After 24 h, take photos again and compare the extent of cell migration between different groups.

Cell proliferation assay

LX-2 cells were plated in 96-well plates at 5,000 cells per well and exposed to either BU or PBS. After 24 h of treatment, 10% CCK-8 solution was added to each well and incubated for 1 h at 37 °C. Absorbance was measured at 450 nm, with results reported as optical density (OD) values.

Butyrate metabolism pathway analysis

The GSE46960 dataset was obtained from the NCBI GEO platform, which includes 64 BA samples and 14 other intrahepatic cholestasis diseases excluding BA as the disease control group. Data preprocessing was carried out as follows: ① If multiple probes map to a single gene, the average value is taken as the expression value; ② Missing values in the data were removed; ③ Data were standardized. Differential gene expression analysis (DEG), along with Gene Ontology (GO), Kyoto Encyclopedia of Genes and Genomes (KEGG), and Gene Set Enrichment Analysis (GSEA), was conducted using the “clusterProfiler” package in R.

Butyrate-Metabolism-Related Genes (BMRGs) were selected (correlation score ≥ 5) and downloaded through the GeneCards database (<http://www.genecards.org>, accessed on 31 March 2022). DEGs-related analysis was performed using the “limma” package in R. The protein-protein interaction (PPI) network for DEGs related to BMRGs was constructed and analyzed using Cytoscape software (v3.9.1), with nodes and edges representing interactions. The STRING database (<https://cn.string-db.org/>) was utilized for interaction analysis, and the MCC algorithm within the “cytohubba” plugin was employed to identify key modules.

Fecal 16S rRNA detection and analysis

Fecal samples (~200 mg per case) were collected aseptically and stored at -80 °C. 16S rRNA sequencing and

bioinformatics analysis were performed by Kingmed Diagnostics (China). DNA was extracted and the V3–V4 hypervariable regions of the 16S rRNA gene were amplified by PCR using modified primers (341 F-805R) with Illumina adapters and barcodes. Paired-end sequencing (2 × 300 bp) was conducted on the Illumina Miseq platform. Raw reads were quality-filtered, assembled into tags, and clustered into OTUs (97% similarity threshold) for taxonomic annotation. Microbial community composition was visualized via relative abundance analysis (Wekemo Bioincloud). Random forest analysis and LEfSe (Galaxy platform) were applied to identify group-specific features. Alpha diversity (Shannon index) and beta diversity (PLS-DA) were analyzed using QIIME2.

Statistics

Statistical analyses were conducted using R software, SPSS 25.0, GraphPad Prism 8.0.1, and ImageJ 1.8.0. Data distribution was initially assessed for normality. For normally distributed continuous variables, results are expressed as mean \pm standard deviation (SD), and inter-group comparisons were performed using the Student's t-test. For comparisons involving more than two groups, one-way analysis of variance (ANOVA) was applied. Non-normally distributed continuous data are presented as median (interquartile range), and the Mann-Whitney U test (rank sum test) was used for group comparisons. Categorical data are expressed as frequencies, and comparisons were conducted using the Chi-square test or Fisher's exact test. A *P* value of < 0.05 was considered statistically significant ($*P < 0.05$, $**P < 0.01$, $***P < 0.001$).

Study approval

The study received ethical approval from the Ethics Committee of Tianjin Children's Hospital (Approval No. 2022-SYYJCYJ-008), and written informed consent was obtained from the legal guardians of each patient. The animal experimental protocols were approved by the Committee on the Ethics of Animal Experiments at Tianjin Medical University.

Results

HDAC2 promotes BA liver fibrosis by activating LX-2 cells

In BA, HDAC2 expression in the liver exhibits a positive correlation with the severity of fibrosis: elevated levels of liver fibrosis are associated with increased HDAC2 expression (Fig. 1A). The activation of HSCs is recognized as a primary driver of liver fibrosis in BA. To further explore the mechanism by which HDAC2 influences liver fibrosis progression in BA, we treated LX-2 cells with the HDACs agonist, ITSA-1. The results demonstrated that the expression of LX-2 activation markers (COL1A1 and α -SMA) was significantly elevated in the ITSA group compared to the control group (Fig. 1B, SFig.

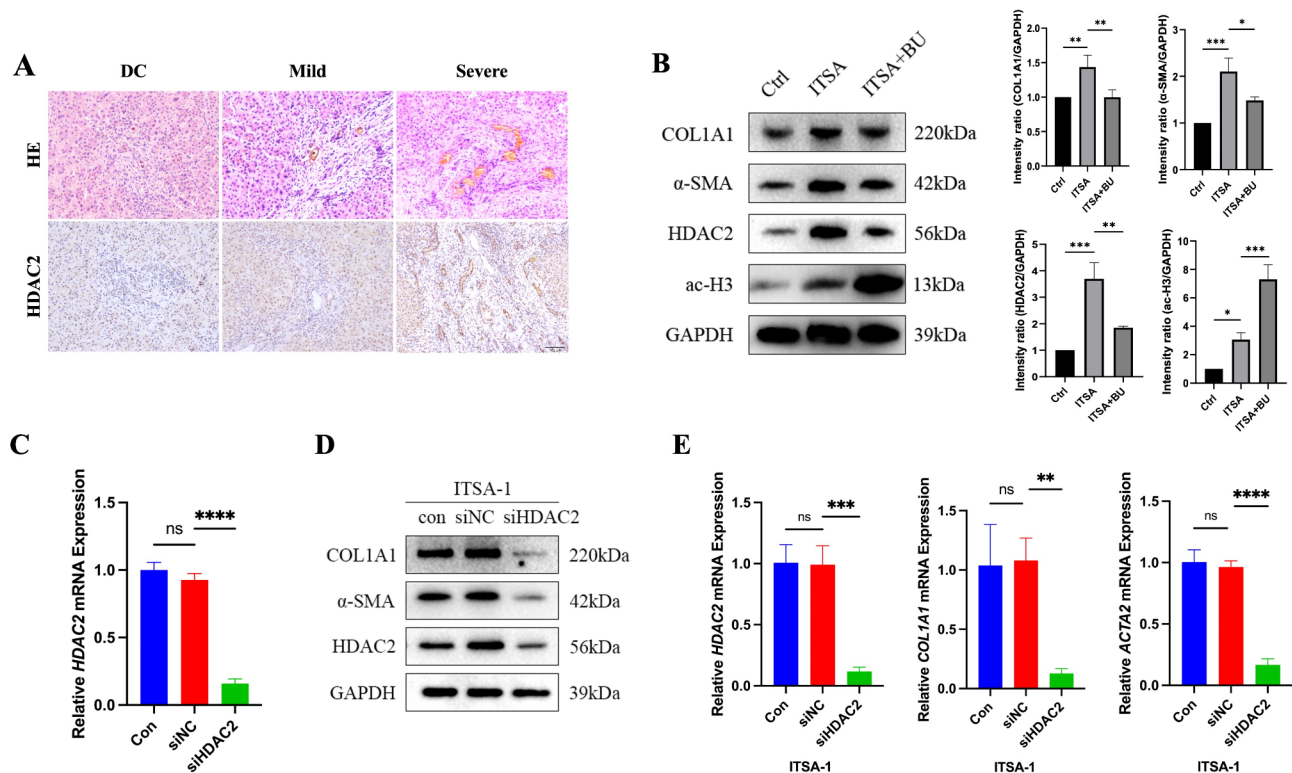


Fig. 1 The Effect of HDAC2 on LX-2 Activation. **(A)** IHC results of HDAC2 protein in liver tissues from disease control group (DC), and mild and severe liver fibrosis in BA. **(B)** Related protein expression after ITSA activation of LX-2 cells. **(C)** qPCR analysis of *HDAC2* mRNA abundance following siRNA-mediated knockdown of *HDAC2*. **(D-E)** LX-2 activation after ITSA intervention in *HDAC2* knockdown cells. WB and qPCR analysis of mRNA abundance and protein expression of LX-2 activation markers. DC, Disease Control; Ctrl, Control Group; ITSA, ITSA intervention in LX-2 cells; ITSA + BU, BU intervention in LX-2 cells activated by ITSA; con, blank control group; siNC, siRNA non-targeting control group; siHDAC2, siHDAC2, LX-2 Knockdown of HDAC2 by siRNA

1A). Next, we knocked down *HDAC2* expression in LX-2 cells using *HDAC2*-siRNA. The siHDAC2 group exhibited significantly reduced HDAC2 gene and protein levels compared to Con group and si-NC groups (S Fig. 1Band C). After ITSA treatment, the expression of LX-2 activation markers in the siHDAC2 group was significantly decreased (Fig. 1D,E). These results suggest that HDAC2 is highly expressed in the liver of BA patients and promotes the development of liver fibrosis. They indicate that HDAC2 may facilitate liver fibrosis by activating LX-2 cells.

Butyrate inhibits LX-2 activation by suppressing HDAC2

Our earlier research has shown an inverse correlation between butyrate levels and BA liver fibrosis, suggesting that butyrate may alleviate liver fibrosis. To investigate this, we treated ITSA-activated LX-2 cells with BU. qPCR, WB, and IF results revealed that, in comparison to the ITSA group, the ITSA + BU group exhibited a marked reduction in the expression of LX-2 activation markers, along with a marked decrease in HDAC2 expression and an increase in histone acetylation levels (Figs. 1B and 2A, B and S Fig. 2A). CCK-8 proliferation assays and cell scratch assays showed that BU significantly inhibited

LX-2 cell proliferation and migration (Fig. 2C and D). These findings suggest that butyrate affects LX-2 activation by inhibiting HDAC2 expression.

Butyrate is closely associated with the IL-6/STAT3 pathway

To further investigate the mechanism by which BU inhibits LX-2 activation, we used the GSE46960 database to intersect 151 DEGs with 993 BMRGs, identifying 22 differentially expressed BMRGs (Fig. 3A and SFig. 3A). Further analysis of key subnetworks revealed the gene *IL6* as a key candidate (Fig. 3B and SFig 3B). GSEA showed that the most significantly affected pathways in BA were the TNF α /NF κ B signaling pathway, epithelial-mesenchymal transition (EMT), inflammation, angiogenesis, and the IL6/JAK/STAT3 signaling pathway. Pathway enrichment analysis further indicated a strong association between IL-6 and butyrate in the context of BA (Fig. 3C, D). Immunohistochemical staining of liver tissues from infants with BA revealed strong positive expression of IL-6 and p-STAT3 (Fig. 3E). This indicates that butyrate is closely associated with the IL-6/STAT3 pathway in BA.

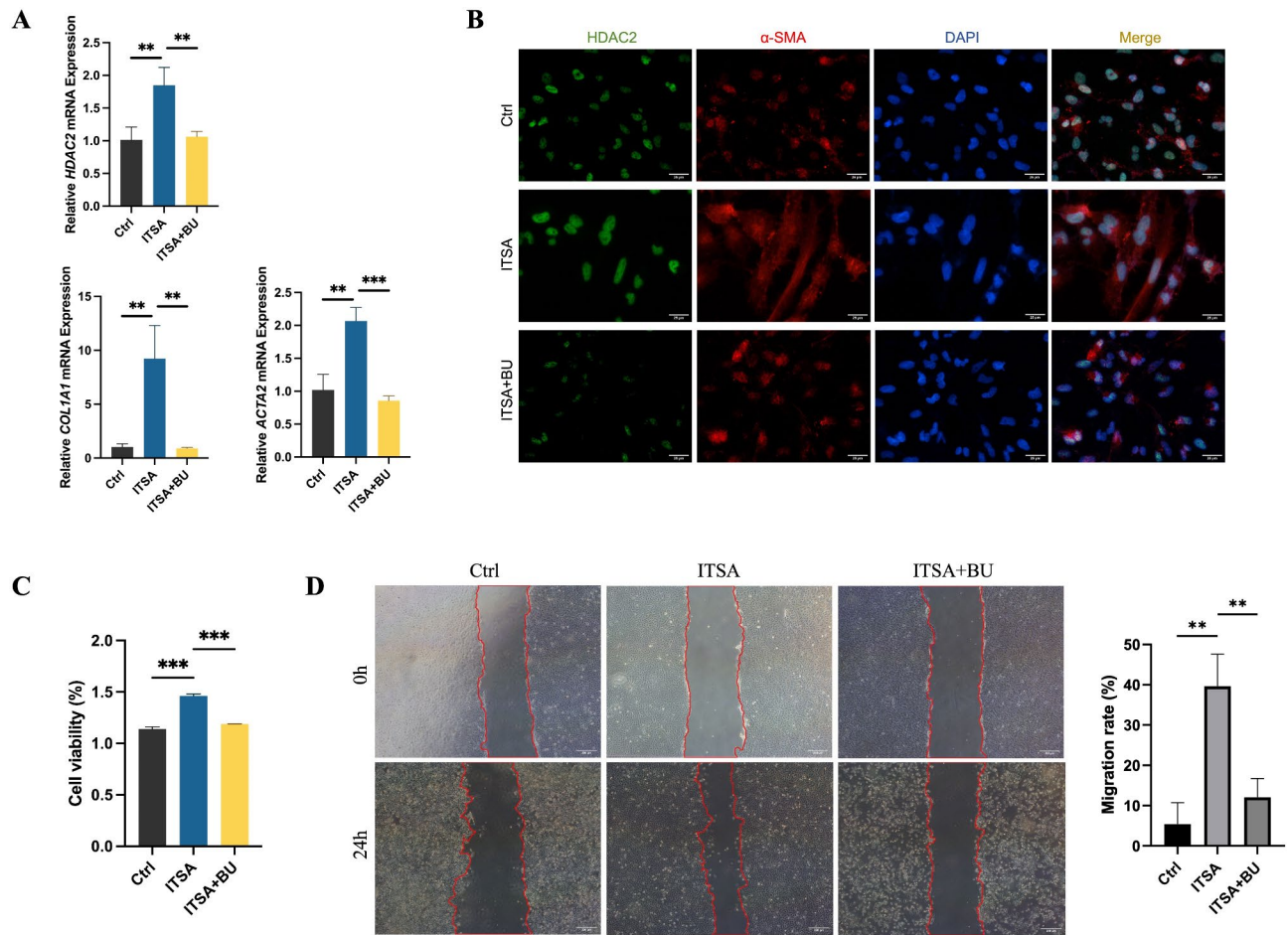


Fig. 2 BU inhibits ITSA-induced activation of LX-2 cells. **(A)** qPCR analysis of mRNA abundance of *HDAC2*, *COL1A1*, and *ACTA2* in LX-2 cells activated by ITSA after BU intervention. **(B)** Immunofluorescence analysis of *HDAC2*, *COL1A1*, and *ACTA2* expression in LX-2 cells activated by ITSA after BU intervention. **(C)** Proliferation analysis of LX-2 cells activated by ITSA after BU intervention. **(D)** Migration analysis of LX-2 cells activated by ITSA after BU intervention

Butyrate inhibits LX-2 activation by regulating the IL-6/STAT3 pathway

After LX-2 cells were activated by ITSA, the expressions of IL-6, p-STAT3, and STAT3 were increased (Fig. 4A, B). This suggests that ITSA activation of LX-2 is associated with the IL-6/STAT3 pathway. To further investigate the relationship, LX-2 cells were pretreated with WP1066, a JAK2/STAT3 pathway inhibitor, prior to ITSA activation. Results indicated that while WP1066 did not affect the expression of HDAC2 or IL-6, it significantly suppressed LX-2 activation (Fig. 4C, D). This indicates that HDAC2 activation of LX-2 is mediated through the IL-6/STAT3 pathway.

Butyrate improves gut microecological environment

To investigate the relationship between BU and liver fibrosis in vivo, BDL mice liver fibrosis model was established (Fig. 5A). Results demonstrated that the BDL group experienced significant weight loss compared to the SHAM and BDL+BU groups (Fig. 5B). Liver injury

markers, such as ALT, were markedly elevated, and liver fibrosis was significantly increased in the BDL group (Fig. 5C, D, E).

16S rRNA sequencing of fecal samples from the three groups revealed significant differences in gut microbiota composition (Fig. 5E, S Fig. 4A). Taxonomic analysis indicated that the gut microbiota composition differed significantly among the groups. Compared to the SHAM group, the BDL group showed an increase in *Firmicutes* and *Proteobacteria* phyla, while *Actinobacteria* and *Bacteroidetes* were reduced. The BU group showed a reduction in *Proteobacteria* and an increase in *Actinobacteria* compared to the BDL group (Fig. 6G, H; S Fig. 4C). These results suggest that the BDL group exhibited dysbiosis with a reduction in beneficial bacteria, which is consistent with microbiota alterations observed in BA patients. However, BU significantly improved the gut microecological environment in the BDL model.

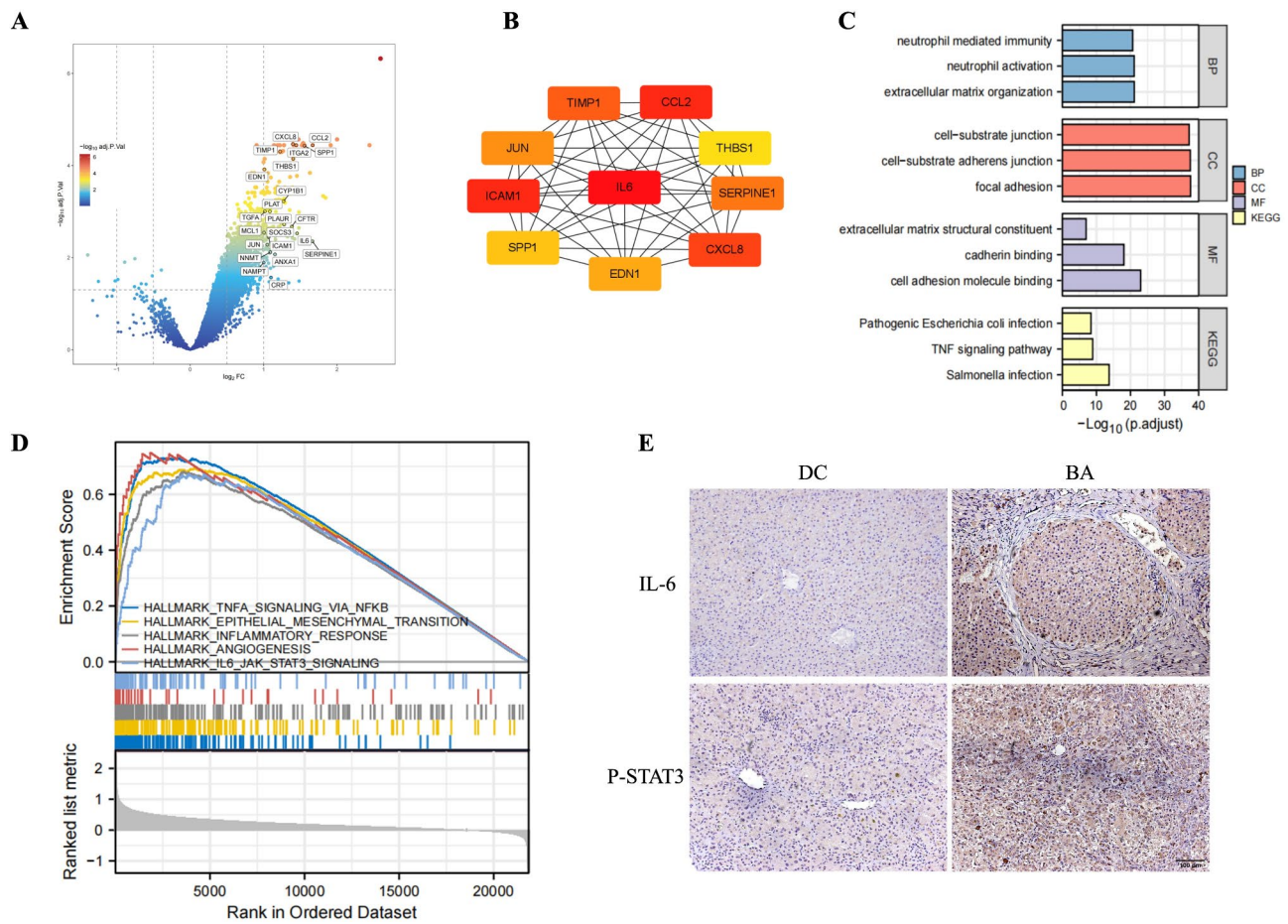


Fig. 3 Butyrate metabolism in BA is associated with the IL6/STAT3 signaling pathway. **(A)** Volcano plot of DEGs highlighting 22 differentially expressed BMRGs from the GSE46960 database. **(B)** Key genes identified from the interaction network using the MCC algorithm in Cytoscape software. **(C)** KEGG and GO enrichment analysis (BA vs. DC). **(D)** GSEA enrichment analysis based on Hallmark gene sets (BA vs. DC). **(E)** Immunohistochemical staining of IL6 and p-STAT3 in BA and CC liver tissues

Butyrate improves BDL mouse liver fibrosis by inhibiting the HDAC2/IL-6/STAT3 pathway

Comparison of the results from the three groups showed that BU significantly improved liver injury and reduced the severity of liver fibrosis in BDL mice (Fig. 5C, D, E). To further investigate the association between BU and the HDAC2/IL-6/STAT3 pathway, qPCR indicated a notable rise in the mRNA abundance of *Hdac2*, *IL-6*, and *Stat3* in BDL mice (Fig. 6A). IF showed that in BDL group, the expression of HDAC2, α -SMA, IL-6, and p-STAT3 were significantly elevated. Moreover, IL-6 and p-STAT3 co-localized with the liver stellate cell marker α -SMA (Fig. 6B). In contrast, in the BU group, the expression levels of HDAC2, α -SMA, IL-6, and p-STAT3 were significantly reduced compared to the BDL group. These findings further suggest that BU alleviates liver fibrosis in BDL mice by inhibiting the activation of the HDAC2/IL-6/STAT3 pathway.

Discussion

In previous studies, we found that infants with BA exhibited a significant reduction in both butyrate-producing microbiota abundance and serum butyrate levels compared to DC [13]. Additionally, we noted a significant increase in HDAC2 protein expression in BA. The expressions of butyrate and HDAC2 were negatively correlated and were both strongly associated with the degree of liver fibrosis. Experimental validation in this study demonstrated that HDAC2 facilitates HSC activation, thus aggravating liver fibrosis. In contrast, butyrate alleviated fibrosis by inhibiting the HDAC2/IL6/STAT3 signaling pathway and improving gut microbiota composition (Fig. 6C).

HDAC2 activation in LX-2 promotes BA liver fibrosis

During the progression of BA, activation of HSCs and portal fibroblasts leads to the continuous accumulation of extracellular matrix (ECM), which drives liver fibrosis progression [19, 20]. The HSCs activation is often

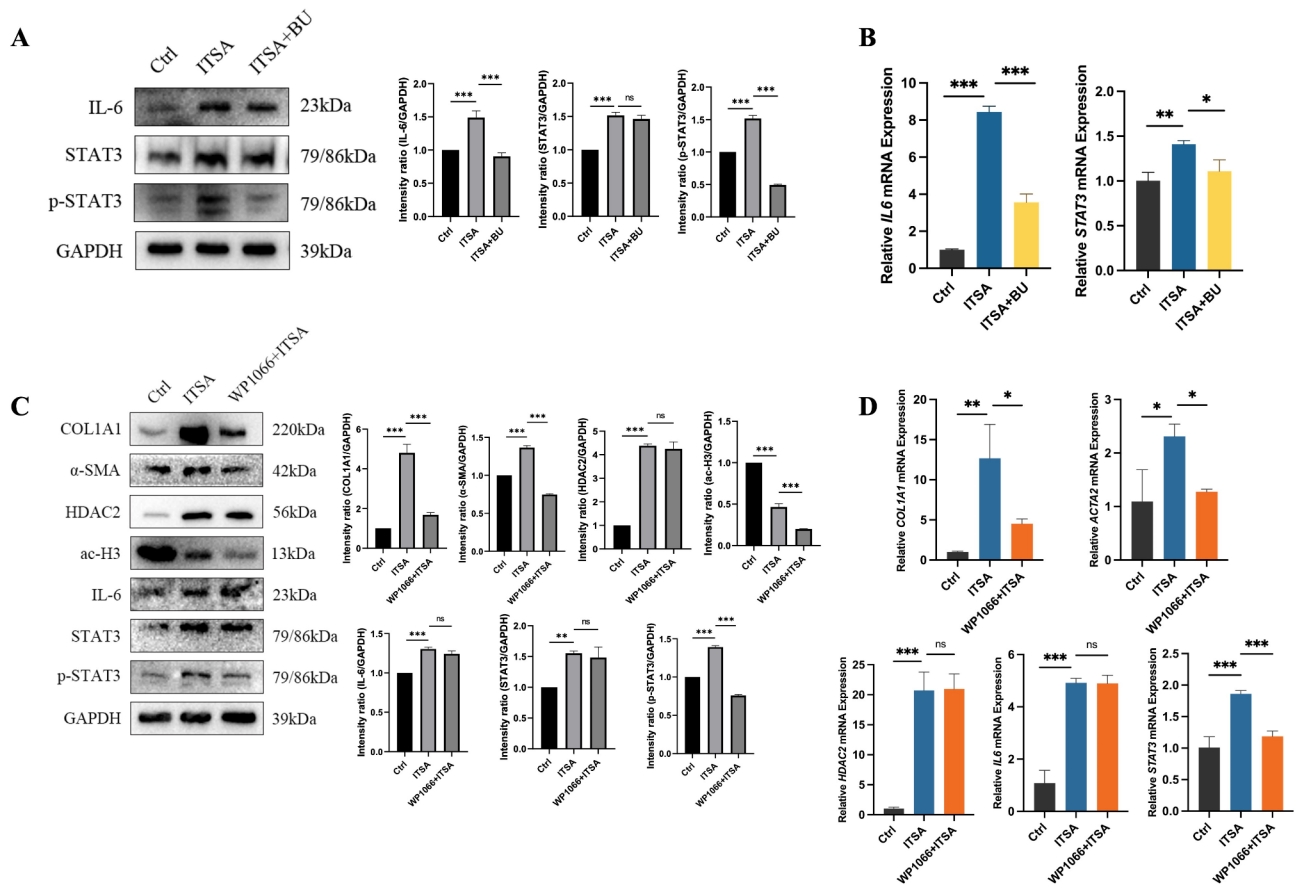


Fig. 4 BU inhibits LX-2 activation by regulating the IL-6/STAT3 pathway. **(A)** Protein expression of IL-6, p-STAT3, and other related proteins in LX-2 cells activated by ITSA after BU intervention. **(B)** qPCR analysis of *IL-6* and *STAT3* gene expression in LX-2 cells activated by ITSA after BU intervention. **(C)** Protein expression of related markers in LX-2 cells activated by ITSA after WP1066 intervention. **(D)** qPCR analysis of related genes in LX-2 cells activated by ITSA after WP1066 intervention

modified by epigenetic modifications, such as DNA methylation and histone deacetylation. While epigenetic studies in BA have primarily focused on DNA methylation and miRNA post-transcriptional regulation, the role of histone acetylation has been less explored, despite its close association with the onset and progression of liver fibrosis [21]. HATs and HDACs jointly regulate protein acetylation. Among the HDAC family, HDAC2, a class I member, deacetylates the N-terminal of histones H3 and H4, resulting in a more compact chromatin structure and gene silencing. HDAC2 is also associated with immune response-related cytokine signaling and is often overexpressed in solid tumors [22, 23]. A study has shown that in CCL4-induced mice models, the mRNA abundance of *Hdac2* is significantly increased [24]. Similarly, our immunohistochemistry results demonstrate a marked increase in HDAC2 expression in the liver tissue of BA patients and BDL mice, correlating with liver fibrosis severity (Figs. 1A and 6A and B). Furthermore, treatment with the HDAC2 agonist ITSA induced LX-2 cell activation and histone deacetylation (Fig. 1B), while silencing HDAC2

expression suppressed LX-2 activation (Fig. 1D, E). These findings suggest that increased HDAC2 expression facilitates LX-2 cell activation, and overexpression of HDAC2 accelerates liver fibrosis in BA.

Butyrate mediates HDAC2 expression to alleviate liver fibrosis

In our previous studies, we observed significant changes in the gut microbiota community and microecological dysbiosis of BA. In comparison to the control group, butyrate-producing bacteria were notably reduced [13]. Butyrate, a key SCFA, relies on gut microbiota composition and abundance for its concentration. Disruption of gut microbiota often reduces butyrate production [25]. Butyrate can pass through the intestinal epithelial barrier and enter the circulation via the portal vein, with circulating butyrate levels reduced in liver cirrhosis. Butyrate exhibits anti-inflammatory, anticancer, and immunomodulatory properties. It can alleviate the progression of various liver diseases, such as primary biliary cholangitis (PBC), nonalcoholic steatohepatitis (NASH),

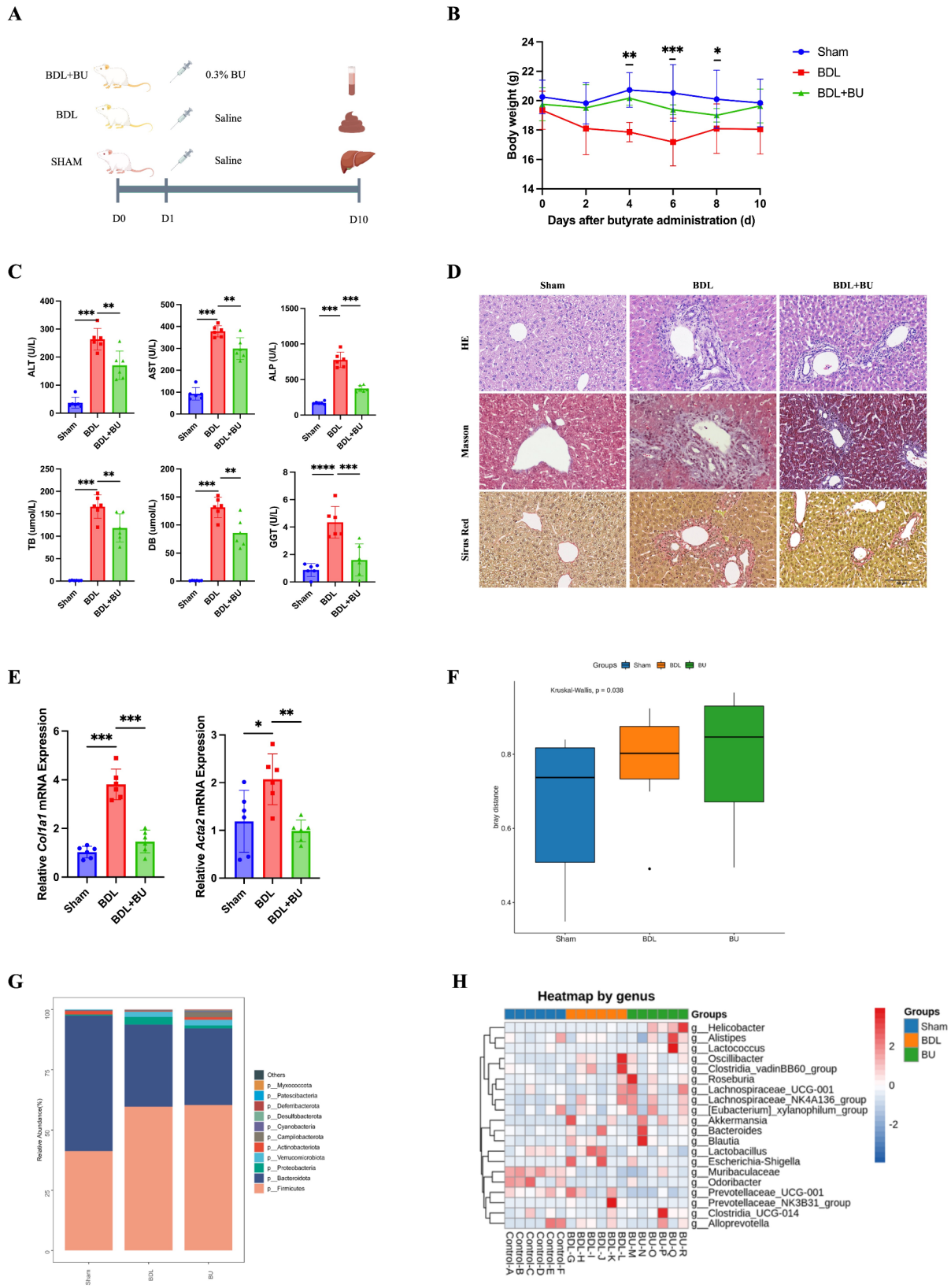


Fig. 5 (See legend on next page.)

(See figure on previous page.)

Fig. 5 BU improves the gut microbiota environment in BDL mice. **(A)** Intervention protocol for Sham, BDL, and BDL+BU groups of mice. **(B)** Weight change curves of mice in the three groups. **(C)** Liver function analysis of mice in the three groups. **(D)** Histological comparison of liver tissues from the three groups of mice using HE, Masson, and Sirius Red staining. **(E)** qPCR analysis of fibrosis markers in liver tissues from the three groups of mice. **(F)** Kruskal-Wallis test analysis of intra-group β -diversity indices in the three groups of mice ($p=0.038$). **(G)** Phylum-level microbiota composition in the three groups of mice. **(H)** Heatmap of the distribution and abundance of key microbial taxa in the three groups of mice

metal toxin-induced liver fibrosis and others [26, 27, 28, 29]. Butyrate can attenuate NASH-related liver fibrosis through the non-canonical TGF- β pathway [17]. And research reported butyrate alleviated cholestasis-induced liver fibrosis by enhancing FGF21 signaling and modulating the gut microbiota [28]. As a HDAC inhibitor, butyrate exerts its effects by inhibiting HDACs and promoting histone acetylation, thereby reducing lysine methylation and increasing acetylation on histone H3, as well as suppressing chromatin transcriptional activity [30]. Butyrate can also reduce cancer cell proliferation, induce differentiation or apoptosis, and modulate gene expression by mediating the inhibition of HDAC activity [31]. However, no study has yet clarified whether butyrate can improve liver fibrosis by inhibiting HDAC2 in BA. In the current investigation, we found treatment with BU significantly decreased HDAC2 expression, increased H3 acetylation levels, and substantially weakened LX-2 cell activation following ITSA-induced activation (Fig. 1B, S Fig. 1A). This suggests that BU may reduce LX-2 activation by inhibiting HDAC2.

Additional in vivo experiments were conducted to further explore the mechanism of butyrate. These studies have demonstrated that butyrate alleviates hepatic steatosis and inflammation, while also hindering the progression of hepatic fibrosis in NASH mice module [17]. In this study, we used BU to intervene in BDL mice model. The results demonstrated that BU significantly improved liver fibrosis and alleviated liver injury in BDL mice (Fig. 5C–E). After BU intervention, HDAC2 expression was notably reduced in the BDL mice (Fig. 6A, B). These findings suggest that BU can also reduce liver fibrosis in the BDL mice by decreasing HDAC2 expression.

Butyrate can improve gut microbiota composition

Through 16S rRNA sequencing to analyze fecal samples from the three groups of mice, we discovered that butyrate significantly alleviated the gut microbiota dysbiosis induced by BDL. The findings revealed that the characteristic microbiota in the Sham group included *Muribaculaceae* and *Odoribacter*, both of which belong to the phylum Bacteroidetes and promote the production of SCFAs. In contrast, *Lactobacillus* and *Shigella* were enriched in the BDL mice; *Shigella* is a clinically common opportunistic pathogen and one of the predominant bacterial genera in cholestatic liver diseases [32]. In the BDL+BU group, the key microbial markers included *Blautia*, *Bifidobacterium*, *Anaerostipes*, and

Akkermansia. *Blautia* is an anaerobic bacterium with probiotic properties, capable of biotransformation and modulating host health, thereby alleviating metabolic diseases and participating in SCFA synthesis [94]. *Akkermansia* can effectively enhance bile acid metabolism and mitochondrial oxidation in the gut-liver axis, improve oxidative stress-induced apoptosis of intestinal cell, and reshape the gut microbiota composition [95]. Notably, *Bifidobacterium*, which is found in maternal vaginal and fecal microbiota, is a primary colonizer promoting neonatal gut health [97]. *Bifidobacterium* can regulate immune responses and produce butyrate, thus enhancing the intestinal barrier and modulating the gut microbiota. Furthermore, the dominant microbiota in the Sham group showed negative correlations with biochemical markers such as ALT, AST, ALP, TB, and DB levels, while the dominant microbiota in the BDL+BU group, *Anaerostipes*, was negatively correlated with ALT, AST, and ALP levels (S Fig. 4D, E). These results provide strong evidence that butyrate not only inhibits liver fibrosis progression in BDL mice but also reshapes the ecological structure of the gut microbiota.

Butyrate regulates HDAC2 through IL-6/STAT3 to ameliorate fibrosis

The study demonstrated that butyrate reduces LX-2 activation by inhibiting HDAC2 expression. To further explore the pathway through which HDAC2 influences LX-2 activation, we performed bioinformatics analysis to identify key genes, revealing that butyrate may act on the IL-6/STAT3 pathway to impact liver fibrosis. IL-6 is a cytokine that exhibits both pro-inflammatory and anti-inflammatory effects, typically produced by activated macrophages. In BA, IL-6 induces the accumulation of inflammatory cells and plays a pivotal role in sustaining both systemic and localized inflammation [33]. Research has shown that the IL-6/STAT3 pathway plays a critical role in HSC activation [34]. Immunohistochemical analysis revealed a significant increase in the expression of both IL-6 and p-STAT3 in the livers of BA and BDL mice (Figs. 3D and 6B), suggesting activation of the IL-6/STAT3 pathway during liver fibrosis in BA. Additionally, we observed that BU suppressed the elevated IL-6/STAT3 signaling following LX-2 activation (Fig. 4A). In a study by Osman et al. [35], it was also noted that butyrate can inhibit the phosphorylation of transcription factors such as NF- κ B, AP1, STAT1, and STAT3. To further verify this, we used the pathway inhibitor WP1066, and

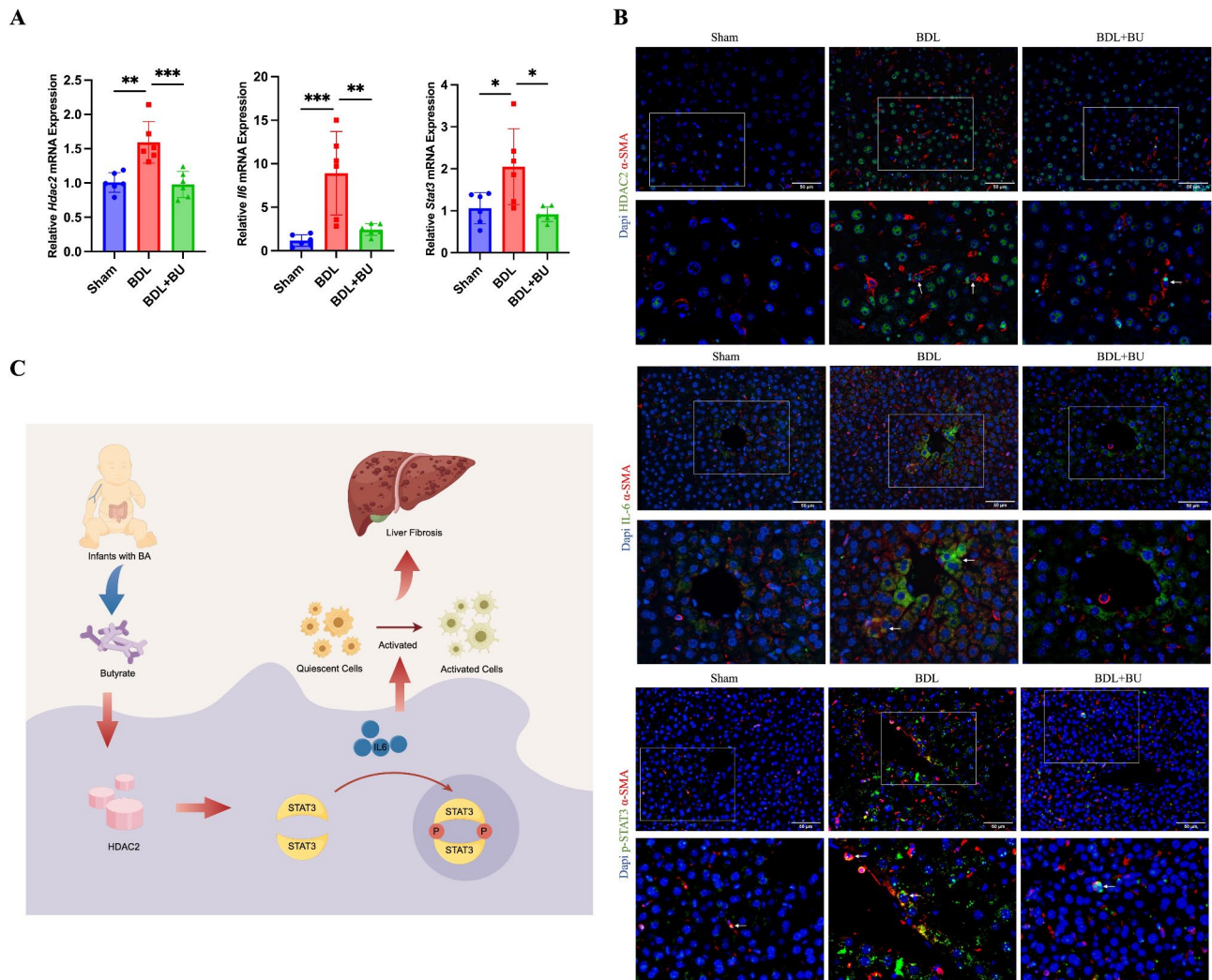


Fig. 6 Butyrate inhibits the HDAC2/IL6/STAT3 pathway and improves liver fibrosis in BDL mice. **(A)** qPCR analysis of *Hdac2*, *Il-6*, and *Stat3* abundance in liver tissues from the three groups of mice. **(B)** Immunofluorescence co-localization results of HDAC2, IL-6, p-STAT3, and α-SMA in liver tissues from the three groups of mice. **(C)** Schematic model depicting the effect of BU on BA liver fibrosis through the HDAC2/IL-6/STAT3 pathway

the combined results from the above experiments demonstrate that butyrate downregulates HDAC2 and suppresses LX-2 activation by modulating the IL-6/STAT3 pathway.

Butyrate plays a significant role in alleviating liver fibrosis in BA. However, butyrate also has side effects [36]. High concentrations of butyrate can inhibit intestinal cell proliferation, activate immune cells, and promote lipid accumulation [37, 38]. To control butyrate release, encapsulation technologies are improving [39]. Clinical studies in patients with liver cancer have found that butyrate intervention increased rates of diarrhea and proteinuria [40]. In clinical trials involving children taking butyrate, some reported side effects such as nausea and headache, which gradually resolved after one month of treatment [41]; while others reported no adverse events [42]. However, there are currently no clinical trials involving infants

aged 0–6 months. Whether butyrate can be used as a therapeutic agent in infants with BA requires further clinical validation.

Conclusion

Based on the analysis of gut microbiota in infants with BA and controls, this study further investigates the mechanisms by which butyrate, a microbial metabolite, influences liver fibrosis in BA. By analyzing the relationship between BA liver fibrosis and histone acetylation at the epigenetic level, we show that butyrate can downregulate HDAC2 expression and inhibit HSCs activation through modulation of the IL-6/STAT3 signaling pathway in both in vitro and in vivo experiments. Our findings suggest that butyrate may play a potential role in suppressing liver fibrosis in BA and improving gut microbiota

structure, providing a new avenue for enhancing the likelihood of NLS in infants with BA.

Abbreviations

BA	Biliary Atresia
HDAC2	Histone Deacetylase 2
BDL	Bile Duct Ligation
NLS	Native Liver Survival
SCFA	Short-Chain Fatty Acid
DC	Disease Controls
HAT	Histone Acetyltransferases
HSC	Hepatic Stellate Cells
OD	Optical Density
DEG	Differential Gene Expression Analysis
GO	Gene Ontology
KEGG	Kyoto Encyclopedia of Genes and Genomes
BMRGs	Butyrate-Metabolism-Related Genes
HDACi	HDAC Inhibitors
NAFLD	Non-Alcoholic Fatty Liver Disease
CC	Choledochal Cysts
BU	Sodium Butyrate
IHC	Immunohistochemical Staining
HRP	Horse Radish Peroxidase
DAB	Diaminobenzidine
IF	Immunofluorescence
GO	Gene Ontology
LefSe	Linear Discriminant Analysis Effect Size
PLS-DA	Partial Least Squares Discriminant Analysis
EMT	Epithelial-Mesenchymal Transition
ECM	Extracellular Matrix

Supplementary Information

The online version contains supplementary material available at <https://doi.org/10.1186/s12887-025-05635-3>.

- Supplementary Material 1:** Supplementary Figure 1
- Supplementary Material 2:** Supplementary Figure 2
- Supplementary Material 3:** Supplementary Figure 3
- Supplementary Material 4:** Supplementary Figure 4
- Supplementary Material 5:** Supplementary Figure Legends
- Supplementary Material 6

Acknowledgements

Not applicable.

Author contributions

Xiaodan Xu and Yilin Zhao designed the research; Yilin Zhao, Xiaodan Xu, Xueting Wang, and Jiayinaxi performed the study; Shaowen Liu and Tengfei Li conducted data mining for public and fecal sequencing data; Liang Ge, Yan Sun, and Shujian Zhang communicated with the families of the patients and collected clinical data and patient specimens; Li Zhao provided pathological interpretation; Yilin Zhao wrote the paper; Xiaodan Xu and Jianghua Zhan supervised the manuscript revision; Jianghua Zhan provided financial support and research guidance.

Funding

Tianjin Municipality Science and Technology Bureau Major Projects (Grant No.21ZXGWSY00070) and Xinjiang Uygur Autonomous Region Science Foundation Projects (Grant No.2022D01A27).

Data availability

Availability of data and materials: Data are available upon request from the corresponding author.

Declarations

Ethics approval and consent to participate

This study was conducted in accordance with the declaration of Helsinki. Informed consent was obtained from all subjects and/or their legal guardian(s). Approval for the research protocol was obtained from the Ethical Committee (2022-SYYJCYJ-008).

Consent for publication

Not applicable.

Competing interests

The authors declare no competing interests.

Received: 27 January 2025 / Accepted: 25 March 2025

Published online: 12 April 2025

References

- Tam PKH, Wells RG, Tang CSM, Lui VCH, Hukkinen M, Luque CD, et al. Biliary Atresia. *Nat Rev Dis Primers*. 2024;10(1):47.
- Bezerra JA, Wells RG, Mack CL, Karpen SJ, Hoofnagle JH, Doo E, et al. Biliary Atresia: clinical and research challenges for the Twenty-First century. *Hepatology*. 2018;68(3):1163–73.
- Hartley JL, Davenport M, Kelly DA. Biliary Atresia. *Lancet*. 2009;374(9702):1704–13.
- Asai A, Miethke A, Bezerra JA. Pathogenesis of biliary Atresia: defining biology to understand clinical phenotypes. *Nat Reviews Gastroenterol Hepatol*. 2015;12(6):342–52.
- Zani A, Quaglia A, Hadzić N, Zuckerman M, Davenport M. Cytomegalovirus-associated biliary Atresia: an aetiological and prognostic subgroup. *J Pediatr Surg*. 2015;50(10):1739–45.
- Ortiz-Perez A, Donnelly B, Temple H, Tiao G, Bansal R, Mohanty SK. Innate immunity and pathogenesis of biliary Atresia. *Front Immunol*. 2020;11.
- Soomro GB, Abbas Z, Hassan M, Luck N, Memon Y, Khan AW. Is there any association of extra hepatic biliary Atresia with cytomegalovirus or other infections? *J Pak Med Assoc*. 2011;61(3):281–3.
- Kasahara M, Umeshita K, Sakamoto S, Fukuda A, Furukawa H, Uemoto S. Liver transplantation for biliary Atresia: a systematic review. *Pediatr Surg Int*. 2017;33(12):1289–95.
- Davis BC, Bajaj JS. The human gut Microbiome in liver diseases. *Semin Liver Dis*. 2017;37(2):128–40.
- Bell DS. Changes seen in gut bacteria content and distribution with obesity: causation or association? *Postgrad Med*. 2015;127(8):863–8.
- Wiest R, Albillos A, Trauner M, Bajaj JS, Jalan R. Targeting the gut-liver axis in liver disease. *J Hepatol*. 2017;67(5):1084–103.
- Wang J, Qian T, Jiang J, Yang Y, Shen Z, Huang Y, et al. Gut microbial profile in biliary Atresia: a case-control study. *J Gastroenterol Hepatol*. 2020;35(2):334–42.
- Xu X, Zhao Y, Wang X, Zhang R, Liu S, Sun R, et al. Diagnostic and prognostic value of the gut microbiota and its metabolite butyrate in children with biliary Atresia. *Pediatr Surg Int*. 2023;40(1):24.
- Eberharter A, Becker PB. Histone acetylation: a switch between repressive and permissive chromatin. Second in review series on chromatin dynamics. *EMBO Rep*. 2002;3(3):224–9.
- Claveria-Cabello A, Colyn L, Arechederra M, Urman JM, Berasain C, Avila MA et al. Epigenetics Liver Fibrosis: Could HDACs Be Therapeutic Target? *Cells*. 2020;9(10).
- Shimazu T, Hirschey MD, Newman J, He W, Shirakawa K, Le Moan N, et al. Suppression of oxidative stress by β -hydroxybutyrate, an endogenous histone deacetylase inhibitor. *Science*. 2013;339(6116):211–4.
- Gart E, van Duyvenvoorde W, Toet K, Caspers MPM, Verschuren L, Nielsen MJ et al. Butyrate protects against Diet-Induced NASH and liver fibrosis and suppresses specific Non-Canonical TGF- β signaling pathways in human hepatic stellate cells. *Biomedicines*. 2021;9(12).
- Xu XD, Wang XT, Liu SW, Zhao YL, Li MD, Zhao L, et al. Relationship between HDAC2 expression score and progression and prognosis of liver fibrosis in biliary Atresia. *Chin J Pediatr Surg*. 2023;44(10):874–81.
- Barcena-Varela M, Colyn L, Fernandez-Barrena MG. Epigenetic mechanisms in hepatic stellate cell activation during liver fibrosis and carcinogenesis. *Int J Mol Sci*. 2019;20(10).

20. Tsukamoto H, Zhu NL, Asahina K, Mann DA, Mann J. Epigenetic cell fate regulation of hepatic stellate cells. *Hepatol Res.* 2011;41(7):675–82.
21. Liu YR, Wang JQ, Huang ZG, Chen RN, Cao X, Zhu DC et al. Histone deacetylase-2: A potential regulator and therapeutic target in liver disease (Review). *Int J Mol Med.* 2021;48(1).
22. Jahan S, Sun JM, He S, Davie JR. Transcription-dependent association of HDAC2 with active chromatin. *J Cell Physiol.* 2018;233(2):1650–7.
23. Krämer OH. HDAC2: a critical factor in health and disease. *Trends Pharmacol Sci.* 2009;30(12):647–55.
24. Li X, Wu XQ, Xu T, Li XF, Yang Y, Li WX, et al. Role of histone deacetylases(HDACs) in progression and reversal of liver fibrosis. *Toxicol Appl Pharmacol.* 2016;306:58–68.
25. Brahe LK, Astrup A, Larsen LH. Is butyrate the link between diet, intestinal microbiota and obesity-related metabolic diseases? *Obes Rev.* 2013;14(12):950–9.
26. Tang J, Zhao H, Li K, Zhou H, Chen Q, Wang H, et al. Intestinal microbiota promoted NiONPs-induced liver fibrosis via effecting serum metabolism. *Ecotoxicol Environ Saf.* 2024;270:115943.
27. Wang R, Li B, Huang B, Li Y, Liu Q, Lyu Z, et al. Gut Microbiota-Derived butyrate induces epigenetic and metabolic reprogramming in Myeloid-Derived suppressor cells to alleviate primary biliary cholangitis. *Gastroenterology.* 2024;167(4):733–e493.
28. Yang J, Chen L, Zhao SS, Du C, Fan YZ, Liu HX, et al. FGF21-dependent alleviation of cholestasis-induced liver fibrosis by sodium butyrate. *Front Pharmacol.* 2024;15:1422770.
29. Zhou D, Pan Q, Xin FZ, Zhang RN, He CX, Chen GY, et al. Sodium butyrate attenuates high-fat diet-induced steatohepatitis in mice by improving gut microbiota and Gastrointestinal barrier. *World J Gastroenterol.* 2017;23(1):60–75.
30. Liu H, Wang J, He T, Becker S, Zhang G, Li D, et al. Butyrate: A Double-Edged sword for health?? *Adv Nutr.* 2018;9(1):21–9.
31. Donohoe DR, Collins LB, Wali A, Bigler R, Sun W, Bultman SJ. The Warburg effect dictates the mechanism of butyrate-mediated histone acetylation and cell proliferation. *Mol Cell.* 2012;48(4):612–26.
32. Shen F, Zheng RD, Sun XQ, Ding WJ, Wang XY, Fan JG. Gut microbiota dysbiosis in patients with non-alcoholic fatty liver disease. *Hepatobiliary Pancreat Dis Int.* 2017;16(4):375–81.
33. Zhang K, Chen Y, Zheng Z, Tang C, Zhu D, Xia X, et al. Relationship between the expression levels of CD4 + T cells, IL-6, IL-8 and IL-33 in the liver of biliary Atresia and postoperative cholangitis, operative age and early jaundice clearance. *Pediatr Surg Int.* 2022;38(12):1939–47.
34. Kong X, Horiguchi N, Mori M, Gao B. Cytokines and stats in liver fibrosis. *Front Physiol.* 2012;3:69.
35. Mohamed Elfadil O, Mundi MS, Abdelmagid MG, Patel A, Patel N, Martindale R. Butyrate: more than a short chain fatty acid. *Curr Nutr Rep.* 2023;12(2):255–62.
36. Yu H, Li R, Huang H, Yao R, Shen S. Short-Chain fatty acids enhance the lipid accumulation of 3T3-L1 cells by modulating the expression of enzymes of fatty acid metabolism. *Lipids.* 2018;53(1):77–84.
37. Kaiko GE, Ryu SH, Koues OI, Collins PL, Solnica-Krezel L, Pearce EJ, et al. The colonic crypt protects stem cells from Microbiota-Derived metabolites. *Cell.* 2016;165(7):1708–20.
38. Kespohl M, Vachharajani N, Luu M, Harb H, Pautz S, Wolff S, et al. The microbial metabolite butyrate induces expression of Th1-Associated factors in CD4(+) T cells. *Front Immunol.* 2017;8:1036.
39. Li J, Mu Y, Liu Y, Kishimura A, Mori T, Katayama Y. Effect of size and loading of retinoic acid in Polyvinyl butyrate nanoparticles on amelioration of colitis. *Polym (Basel).* 2021;13(9).
40. Nouse K, Shiota S, Fujita R, Wakuta A, Kariyama K, Hiraoka A, et al. Effect of butyrate-producing Enterobacteria on advanced hepatocellular carcinoma treatment with Atezolizumab and bevacizumab. *Cancer Med.* 2023;12(17):17849–55.
41. Coppola S, Nocerino R, Paparo L, Bedogni G, Calignano A, Di Scala C, et al. Therapeutic effects of butyrate on pediatric obesity: A randomized clinical trial. *JAMA Netw Open.* 2022;5(12):e2244912.
42. Pietrzak A, Banasiuk M, Szczepanik M, Borys-Iwanicka A, Pytrus T, Walkowiak J et al. Sodium butyrate effectiveness in children and adolescents with newly diagnosed inflammatory bowel Diseases-Randomized Placebo-Controlled multicenter trial. *Nutrients.* 2022;14(16).

Publisher's note

Springer Nature remains neutral with regard to jurisdictional claims in published maps and institutional affiliations.